The Plant Cell, Vol. 15, 2503–2513, November 2003, www.plantcell.org © 2003 American Society of Plant Biologists

RESEARCH ARTICLES

An Arabidopsis Callose Synthase, GSL5, Is Required for Wound and Papillary Callose Formation

Andrew K. Jacobs,[a,b,1] Volker Lipka,[b,1] Rachel A. Burton,[a] Ralph Panstruga,[b] Nicolai Strizhov,[c] Paul Schulze-Lefert,[b,2] and Geoffrey B. Fincher[a]

[a] Australian Centre for Plant Functional Genomics, University of Adelaide, Waite Campus, Glen Osmond, South Australia 5064, Australia

[b] Department of Plant Microbe Interactions, Max-Planck-Institute for Plant Breeding Research, D-50892 Cologne, Germany

[c] Max-Planck-Unit for Structural Molecular Biology, 22607 Hamburg, Germany

Arabidopsis was transformed with double-stranded RNA interference (dsRNAi) constructs designed to silence three putative callose synthase genes: *GLUCAN SYNTHASE–LIKE5* (*GSL5*), *GSL6*, and *GSL11*. Both wound callose and papillary callose were absent in lines transformed with *GSL5* dsRNAi and in a corresponding sequence-indexed *GSL5* T-DNA insertion line but were unaffected in *GSL6* and *GSL11* dsRNAi lines. These data provide strong genetic evidence that the *GSL* genes of higher plants encode proteins that are essential for callose formation. Deposition of callosic plugs, or papillae, at sites of fungal penetration is a widely recognized early response of host plants to microbial attack and has been implicated in impeding entry of the fungus. Depletion of callose from papillae in *gsl5* plants marginally enhanced the penetration of the grass powdery mildew fungus *Blumeria graminis* on the nonhost Arabidopsis. Paradoxically, the absence of callose in papillae or haustorial complexes correlated with the effective growth cessation of several normally virulent powdery mildew species and of *Peronospora parasitica*.

INTRODUCTION

Callose is a (1→3)-β-D-glucan that is widely distributed in higher plants and is readily recognizable in tissue sections through the formation of an intense yellow, UV light–induced fluorescence with the aniline blue fluorochrome (Stone et al., 1985). During normal plant growth and development, callose is found as a transitory component of the cell plate in dividing cells, is a major component of pollen mother cell walls and pollen tubes, and is found as a structural component of plasmodesmatal canals. Callose also has been observed in abscission zones and on sieve plates in dormant phloem (Stone and Clarke, 1992).

In addition to its role in normal growth and development, callose is deposited between the plasma membrane and the cell wall after exposure of plants to a range of abiotic and biotic stresses, including wounding, desiccation, metal toxicity, and microbial attack (Stone and Clarke, 1992). Particular attention has been focused on callose formation in plant–microbe interactions, during which plant host cells respond to microbial attack by rapidly synthesizing and depositing callose as plugs, drops, or plates in close proximity to the invading pathogen (Ryals et al., 1996; Donofrio and Delaney, 2001). These callosic deposits are commonly referred to as papillae and are thought to contain, in addition to (1→3)-β-D-glucan, minor amounts of other polysaccharides, phenolic compounds, reactive oxygen intermediates, and proteins (Smart et al., 1986; Bolwell, 1993; Bestwick et al., 1997; Thordal-Christensen et al., 1997; Heath, 2002). Although the precise function of callosic papillae during microbial attack has not been demonstrated unequivocally, it has been postulated that the papillae act as a physical barrier to impede microbial penetration (reviewed by Stone and Clarke, 1992). By slowing or immobilizing the invading microorganisms, the host plant could focus upon them a number of antimicrobial compounds, such as wall-degrading enzymes, phytoalexins, and active oxygen species, or initiate cascade responses involving race-specific resistance genes (Brown et al., 1998).

The central importance of callose deposition in several key plant processes, both under normal growth conditions and after abiotic or biotic stress, has prompted many attempts to purify and characterize callose synthases from plants. To date, no highly purified callose synthase preparations have been reported; therefore, it has not been possible to demonstrate a direct link between callose synthase activity and amino acid or nucleotide sequence. Nevertheless, evidence is accumulating that callose synthases are encoded by a family of glucan synthase–like (*GSL*) genes (Cui et al., 2001; Doblin et al., 2001; Hong et al., 2001a; Østergaard et al., 2002), based on the homology of these plant genes with yeast *FK506 hypersensitivity* (*FKS*) genes, which also are believed to be involved in (1→3)-β-D-glucan biosynthesis (Douglas et al., 1994; Cabib et al., 2001; Dijkgraaf et al., 2002).

[1] These authors contributed equally to this report.

[2] To whom correspondence should be addressed. E-mail schlef@mpiz-koeln.mpg.de; fax 49-221-5062313.

Article, publication date, and citation information can be found at www.plantcell.org/cgi/doi/10.1105/tpc.016097.

Twelve *GSL* genes have been identified in Arabidopsis (Richmond and Somerville, 2000; Verma and Hong, 2001; http://cellwall.stanford.edu/), in which individual members of the family presumably mediate the synthesis of callose in different tissues and/or under different environmental conditions. Very limited information is available about the biological functions of individual AtGSL family members. GSL6 (CalS1) is located at the growing cell plate and interacts with two cell plate–associated proteins, phragmoplastin and a UDP-glucose transferase (Hong et al., 2001a, 2001b). The three proteins likely form part of a larger complex that assembles at the cell plate (Hong et al., 2001b). Transgenic tobacco lines overexpressing a *GREEN FLUORESCENT PROTEIN* (*GFP*)–*AtGSL6* construct showed increased callose deposition at the cell plate, but this gene failed to complement the yeast mutant *fks1* (Hong et al., 2001a). *AtGSL5* has been shown to partially complement *fks1* and is inducible by salicylic acid (Østergaard et al., 2002). Despite these observations, direct genetic evidence linking *GSL* genes to callose biosynthesis in plants generally, or genetic evidence linking individual *AtGSL* family members to specific sites of callose deposition in Arabidopsis, has yet to be found.

The work described here was initiated in an attempt to identify members of the Arabidopsis *GSL* gene family that might be upregulated after wounding and when Arabidopsis leaves are exposed to the powdery mildew fungus *Blumeria graminis*. This ascomycete is a common fungal pathogen of grasses but fails to produce disease in nonhost interactions with Arabidopsis or other dicot plants (Braun et al., 2002). Semiquantitative reverse transcriptase–mediated PCR indicated that, of the 12 Arabidopsis *GSL* genes, transcript levels for *GSL5*, *GSL6*, and *GSL11* increased slightly after inoculation of leaves with *B. graminis* spores; on this basis, these genes were chosen for further examination (our unpublished data). Here, we assign the GSL5 isoform (referred to as CalS12 by Hong et al. [2001a]) a crucial role in inducible callose accumulation upon wounding and during biotic stress. Contrary to the common belief that callose accumulation contributes to plant defenses against pathogen attack, our data indicate that callose synthesized by the wound-responsive GSL5 might protect the fungus during pathogenesis.

RESULTS

GSL Transcript Levels Are Reduced in Double-Stranded RNA Interference Lines

Fertile transgenic T3 Arabidopsis lines were obtained for each of the three double-stranded RNA interference (dsRNAi) constructs, which targeted *GSL5*, *GSL6*, and *GSL11*. The *GSL5*, *GSL6*, *GSL11*, and empty vector control lines exhibited no obvious morphological abnormalities. DNA gel blot hybridization analyses confirmed the presence of the dsRNAi construct in each line, most of which carried single copies of the transgene (data not shown). When total RNA was extracted from young leaves and inflorescences of dsRNAi lines for quantitative real-time PCR analysis, mRNA for the three *GSL* genes was generally 3- to 10-fold less abundant than in the empty vector controls and wild-type lines (Figure 1).

Wound and Papillary Callose Are Reduced in *GSL5* dsRNAi Transgenic Lines

The formation of wound callose in *GSL5* dsRNAi lines was greatly reduced or absent compared with that in the *GSL6*, *GSL11*, and control lines (Figure 2). When germinated pollen

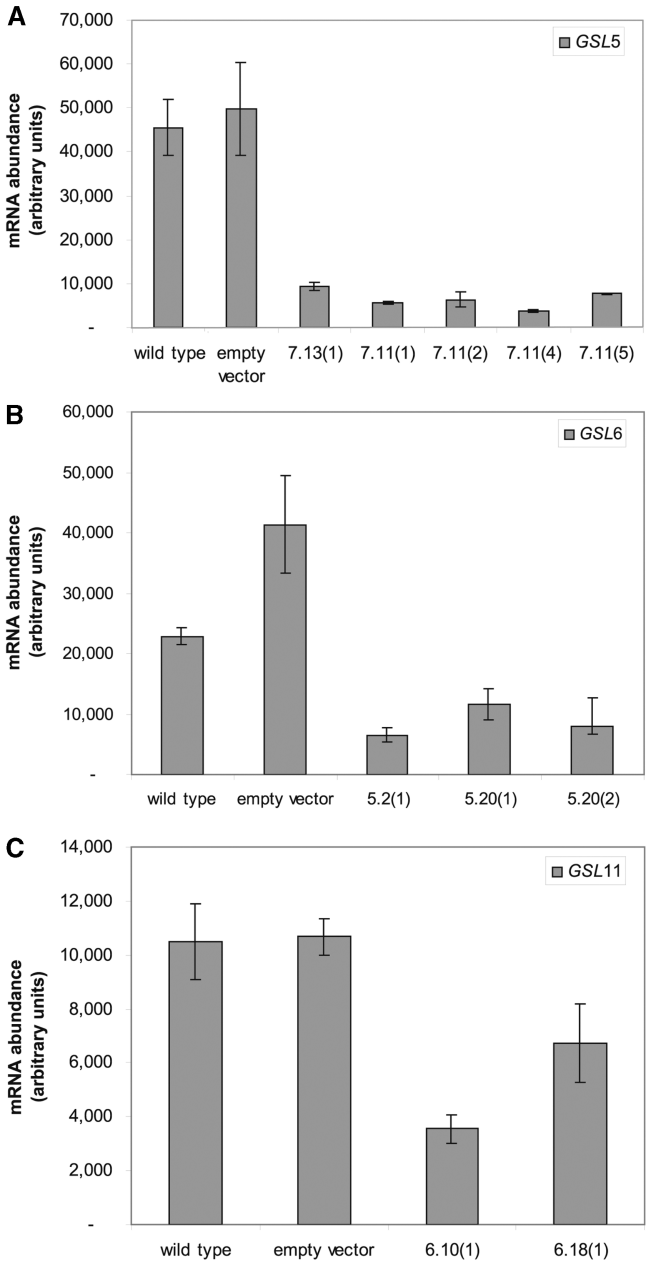

Figure 1. Transcript Accumulation of *GSL* Genes Is Reduced in Transgenic dsRNAi Lines.

Quantitative analysis of mRNA steady state levels showed a significant reduction of *GSL* transcript accumulation in transgenic lines harboring dsRNAi constructs directed against *GSL5* [lines 7.13(1), 7.11(1), 7.11(2), 7.11(4), and 7.11(5)] **(A)**, *GSL6* [lines 5.2(1), 5.20(1), and 5.20(2)] **(B)**, or *GSL11* [lines 6.10(1) and 6.18(1)] **(C)**.

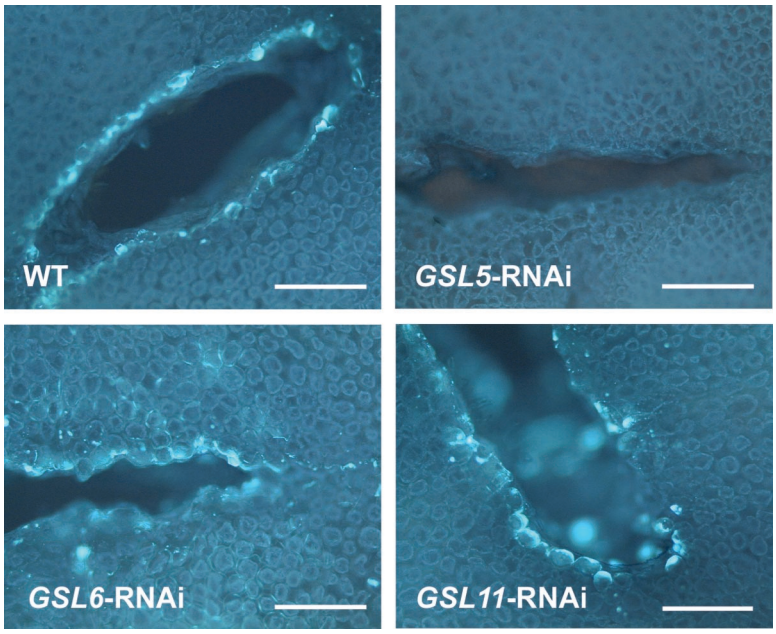

Figure 2. Reduced Callose Accumulation at Wound Sites in *GSL5* dsRNAi Lines.

Leaves of wild-type (WT) plants and *GSL5*, *GSL6*, and *GSL11* dsRNAi lines were wounded by cutting with a razor. Aniline blue fluorochrome staining of leaves revealed reduced callose accumulation at wound sites after 24 h. Bars = 200 μm.

grains in the three dsRNAi transgenic lines were examined with the aniline blue fluorochrome, callosic deposits in the *GSL5* line appeared normal (data not shown). No differences were observed in any of the *GSL* dsRNAi lines for cell plate or plasmodesmata callose (data not shown).

Given that fungal penetration is likely to cause wounding of plant cells, the formation of callosic plugs was examined in transgenic *GSL* dsRNAi lines after inoculating leaves with spores from the virulent powdery mildew fungus *Sphaerotheca fusca*. Elongating fungal hyphae were observed in all cases, and the rate of hyphal growth on the leaf surface did not differ substantially between the lines for at least 48 h after inoculation. Callosic papillae that stained brightly with the aniline blue fluorochrome were clearly evident in all independent *GSL6*, *GSL11*, and control lines (Figure 3). By contrast, in all independent *GSL5* transgenic lines, callosic plugs were completely absent, despite the fact that hyphal growth occurred (Figure 3).

Wound and Papillary Callose Also Are Reduced in a *GSL5* T-DNA Insertion Line

To confirm that the effects in the *GSL5* dsRNAi lines were specific to the lack of the GSL5 callose synthase isoform, we examined a T-DNA insertion line (GABI-KAT 089H05) containing an insertion in the second exon of *GSL5*. When leaves of homozygous T-DNA insertion siblings (referred to as *gsl5-1*) were wounded or inoculated with *S. fusca*, they showed similar, dramatic reductions in wound callose and papillary callose formation (data not shown).

Inoculation with conidiospores of the *B. graminis* powdery mildew failed to produce disease on wild-type Arabidopsis leaves. Microscopic examination revealed normal conidiospore germination, with production of primary and differentiated appressorial germ tubes in contact with the leaf surface. However, the germ tubes typically failed to enter the nonhost epidermal cells (92% of interaction sites) and were accompanied by the formation of callosic papillae (Figures 4A to 4C). This infection phenotype is similar to other reported nonhost interactions between plants and fungal pathogens (Kobayashi et al., 1997; Heath, 2002). By contrast, callosic plugs were virtually undetectable in both the homozygous *GSL5* T-DNA insertion line (*gsl5-1*) and the *GSL5* dsRNAi lines (Figures 4B and 4C). *B. graminis* penetration indices were only slightly higher in *gsl5-1* than in wild-type plants (Figure 4A), suggesting that callose plays a minor role in resistance to wall penetration. In T2 progeny obtained after selfing of the GABI-KAT 089H05 T1 line, which was hemizygous for the T-DNA insertion, siblings homozygous or hemizygous for the T-DNA insertion in *GSL5* cosegregated with the absence or presence of callosic plugs, respectively, beneath *B. graminis* appressoria (Figure 5). Despite the absence of callosic plugs in *gsl5-1* mutant plants, round papillae still were clearly recognizable beneath fungal appressoria (Figure 4C), indicating that components other than callose were present in these subcellular structures.

A cell death response was observed in epidermal cells that were penetrated by *B. graminis* sporelings at ~48 h after spore inoculation (~15% of interaction sites; Figure 4A). In contrast to epidermal cells that were not penetrated by the fungus, com-

plete collapse and browning of cytoplasm was observed in epidermal cells containing haustoria in wild-type and *gsl5-1* genotypes. Cytoplasmic collapse and browning is considered a reliable indicator of cell death (Heath, 1998). Trypan blue staining was used to confirm these observations (data not shown). Cell death was accompanied by an intense aniline blue fluorochrome staining pattern along the entire cell margin in wild-type plants, whereas dead epidermal cells in *gsl5-1* mutants showed only a punctate callose staining pattern at the cell periphery (Figure 4D). The punctate staining pattern in *gsl5-1* plants was reminiscent of plasmodesmata that are known to contain callose (Northcote et al., 1989; Itaya et al., 1998); therefore, we conclude that the absence of heavy GSL5 callose deposition at cell margins in *gsl5-1* plants reveals the underlying plasmodes-

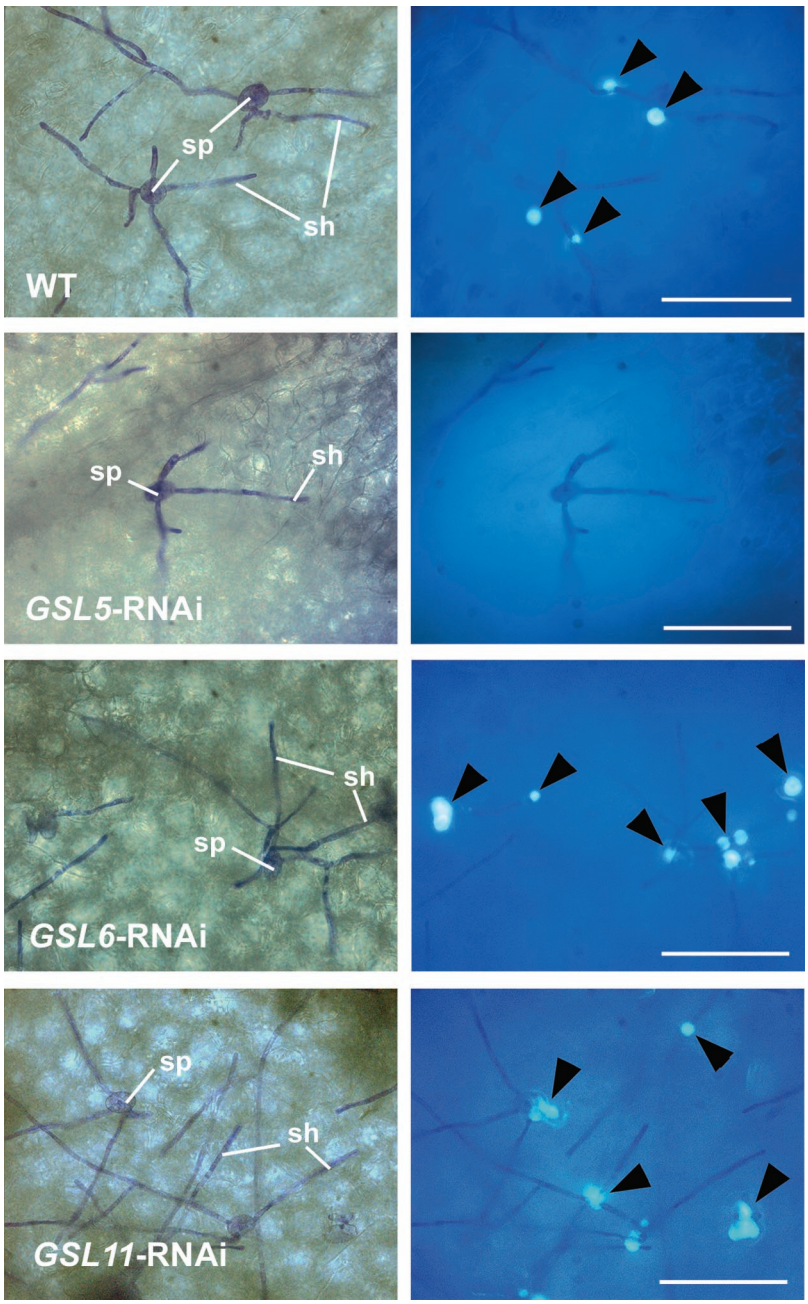

Figure 3. Absence of Callose Accumulation upon Powdery Mildew Infection in *GSL5* dsRNAi Lines.

Leaves of wild-type (WT) plants and *GSL5*, *GSL6*, and *GSL11* dsRNAi lines were challenged with the virulent powdery mildew fungus *S. fusca*. Forty-eight hours after inoculation, fungal structures (left column) and callose deposits in papillae (right column; marked by arrowheads) were stained with Coomassie blue and the aniline blue fluorochrome, respectively. sh, secondary hyphae; sp, conidiospore. Bars = 100 μm.

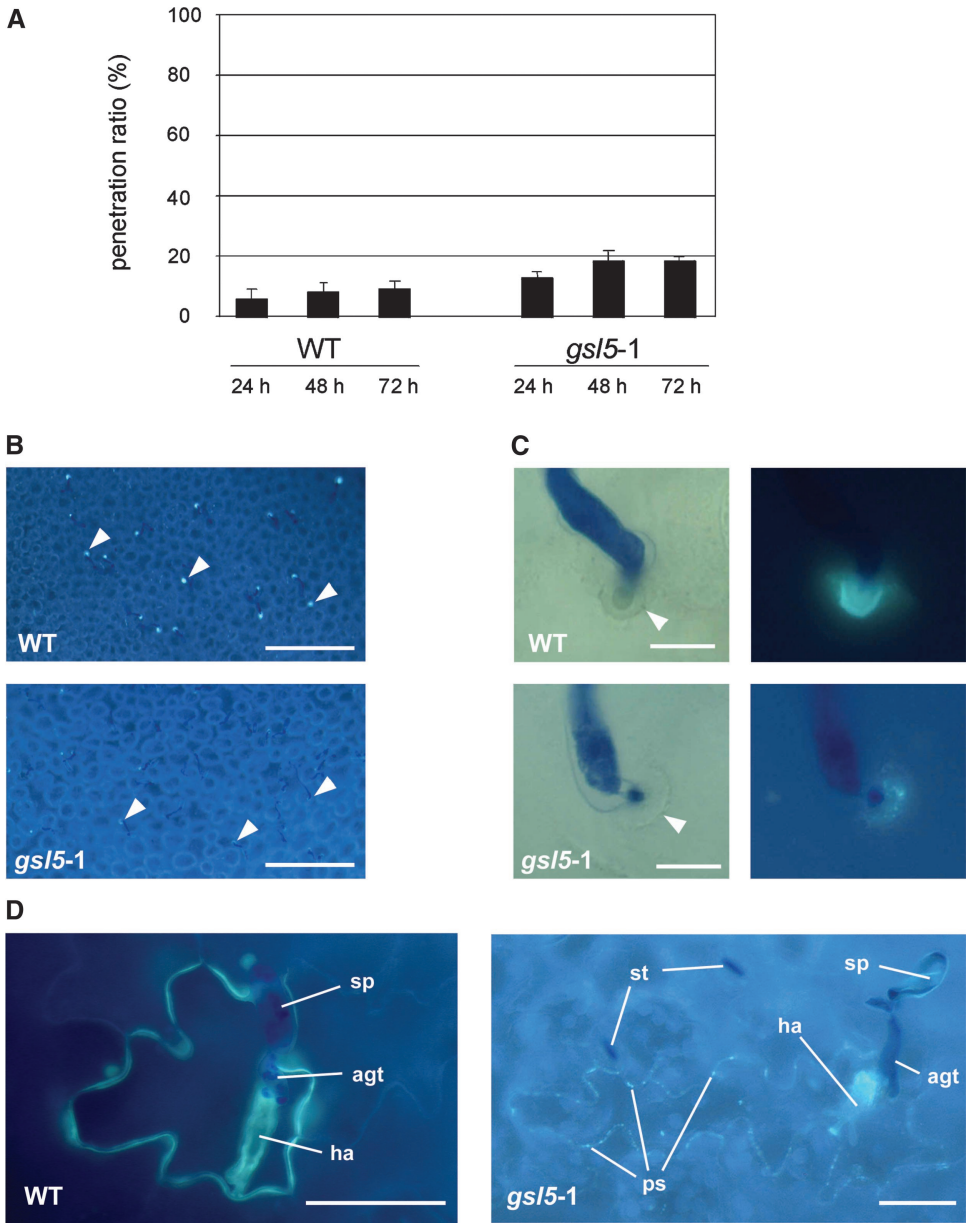

Figure 4. GSL5 Callose Accumulation Patterns upon Challenge with the Grass Powdery Mildew Fungus *B. graminis*.

Wild-type (WT) and T-DNA insertion (*gsl5-1*) plants were inoculated with *B. graminis* f. sp. *hordei* conidiospores.

(A) Quantitative analysis of *B. graminis* penetration rate. At least 300 interaction sites between *B. graminis* sporelings and leaf epidermal cells were scored for the presence or absence of fungal haustoria at the times indicated.

(B) Callose depositions at sites of attempted *B. graminis* cell wall penetration (arrowheads) are visible by fluorescence microscopy on wild-type but not *gsl5-1* plants 24 h after inoculation. Bars = 200 μm.

(C) Higher magnification views of papillae (arrowheads) beneath fungal appressoria in wild-type (top row) and *gsl5-1* (bottom row) plants. Light microscopy images are shown at left, and corresponding fluorescence images after aniline blue fluorochrome staining are shown at right. Bars = 10 μm.

(D) Invasive growth of *B. graminis* (successful haustorium differentiation) in single epidermal cells of wild-type leaves leads to cell death and callose deposition along the entire cell margin. Fluorescence images were taken 48 h after inoculation, and leaves were stained with the aniline blue fluorochrome. Note the relatively low-intensity punctate fluorochrome staining pattern at the cell periphery in *gsl5-1* plants. agt, appressorial germ tube; ha, haustorium; ps, punctate staining; sp, conidiospore; st, stomata. Bars = 50 μm.

mata callose. This finding indicates that massive GSL5 callose accumulation normally occurs along the cell margin during pathogen-triggered cellular suicide and that the GSL5 cell margin callose and the plasmodesmata callose are synthesized by different callose synthase isoforms of the same cell.

The Mutant *powdery mildew resistant4-1* Contains a Defective *GSL5* Gene

The Arabidopsis mutant *powdery mildew resistant4-1* (*pmr4-1*) was shown previously to be resistant against *Erysiphe cichoracearum* and to lack callose at fungal penetration sites; the recessive mutation was mapped to the long arm of chromosome 4 (Vogel and Somerville, 2000). We noticed that *GSL5* is located in the same chromosomal region and tested whether *pmr4-1* might contain a mutation in *GSL5*. Direct DNA sequencing revealed a single base substitution (G→A) in genomic DNA of *pmr4-1* corresponding to position 2060 in the deduced coding sequence, whereas the sequence derived from wild-type plants was identical to the *GSL5* gene in the databases. The base substitution would result in the conversion of the TGG codon for Trp-687 in *GSL5* to a TAG stop codon and the formation of a severely truncated primary translation polypeptide of 686 amino acid residues. The position of the lesion in *GSL5* of the *pmr4-1* mutant line is compared with the position of the T-DNA insertion in the GABI-KAT 089H05 line in Figure 6.

GSL5 and *PMR4* Are the Same Gene

Mutant *pmr4-1* plants were reported previously to exhibit resistance against *E. cichoracearum* and the oomycete *Peronospora parasitica* (Vogel and Somerville, 2000). We challenged *pmr4-1*, *gsl5-1*, and the GSL5 dsRNAi lines with another virulent powdery mildew species, *Golovinomyces orontii*. In contrast to susceptible wild-type Arabidopsis, comparable enhanced disease resistance was observed (Figure 7A), indicating that the absence of *PMR4* or *GSL5* confers similar broad-spectrum resistance. When *pmr4-1* plants were inoculated with *B. graminis* spores, the infection phenotype was indistinguishable from that observed in the *AtGSL5* dsRNAi and *gsl5-1* plants, and callosic papillae were not detected (see above). To determine whether *PMR4* and *GSL5* might be the same gene, we crossed the homozygous T-DNA insertion line (*gsl5-1*) with the *pmr4-1* mutant. Inspection of 15 F1 plants after fungal spore inoculation with the virulent *G. orontii* powdery mildew showed enhanced disease resistance and lack of callose accumulation at attempted infection sites. The observed infection phenotypes of the F1 plants were indistinguishable from the *pmr4-1* and *gsl5-1* parental lines (data not shown), strongly indicating that *PMR4* and *GSL5* are the same gene.

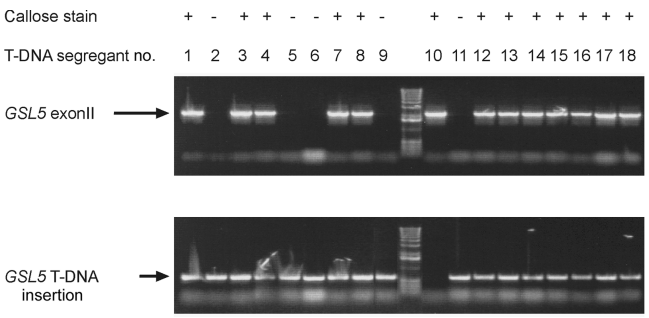

Figure 5. Lack of Callose Deposition Cosegregates with T-DNA Insertion in *GSL5*.

Absence of aniline blue fluorochrome staining after inoculation with *B. graminis* correlates with a homozygous T-DNA insertion (ins.) in *GSL5*. Segregating progeny (18 T2 siblings) of a selfed hemizygous T-DNA *GSL5* insertion line were genotyped molecularly and tested for callose deposition upon challenge with *B. graminis*. Gel electrophoretic separation of PCR products obtained with a *GSL5*– and T-DNA–specific oligonucleotide primer indicated the presence of the T-DNA insertion in all individuals except sibling 10 (bottom gel). The absence of a PCR amplification product using oligonucleotide primers designed to bind on either side of the T-DNA insertion site in *GSL5* exon 2 demonstrated that siblings 2, 5, 6, 9, and 11 are homozygous for the T-DNA insertion (top gel).

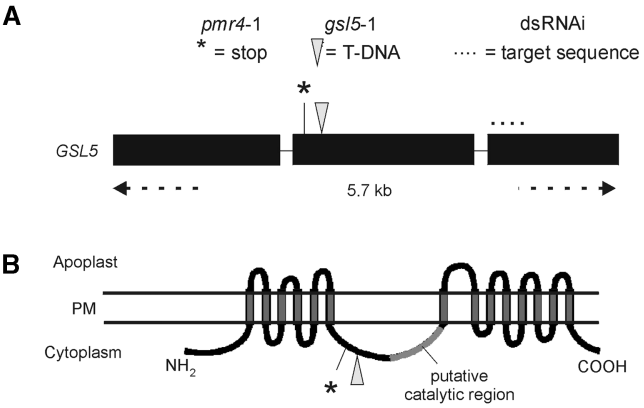

Figure 6. Scheme of *GSL5* Gene Structure and Deduced GSL5 Protein Topology.

(A) *GSL5* gene structure. Black boxes represent exons, and lines indicate introns. The asterisk indicates the mutation site in *pmr4-1* that generates a stop codon. The gray triangle represents the T-DNA insertion site in the GABI-KAT 089H05 line (*gsl5-1*). The dotted line above exon 3 shows the target sequence used to generate the *GSL5* dsRNAi construct.

(B) GSL5 is predicted to be a polytopic integral membrane protein with ~14 transmembrane helices. Both the NH_2 and COOH termini are predicted to be orientated toward the cytoplasm, as is the putative catalytic domain, which is located in an extended loop between predicted transmembrane helices 6 and 7. Mutation sites in *pmr4-1* and *gsl5-1* are indicated as described in **(A)**. PM, plasma membrane.

GSL5 Is Required for Callose Encasement of Haustorial Complexes

We examined the enhanced disease resistance phenotype to *G. orontii* (Figure 7A) in greater detail at the microscopic level (Figures 7B to 7D). This revealed indistinguishable hyphal growth on wild-type and *gsl5-1* leaves at 72 h after spore inoculation

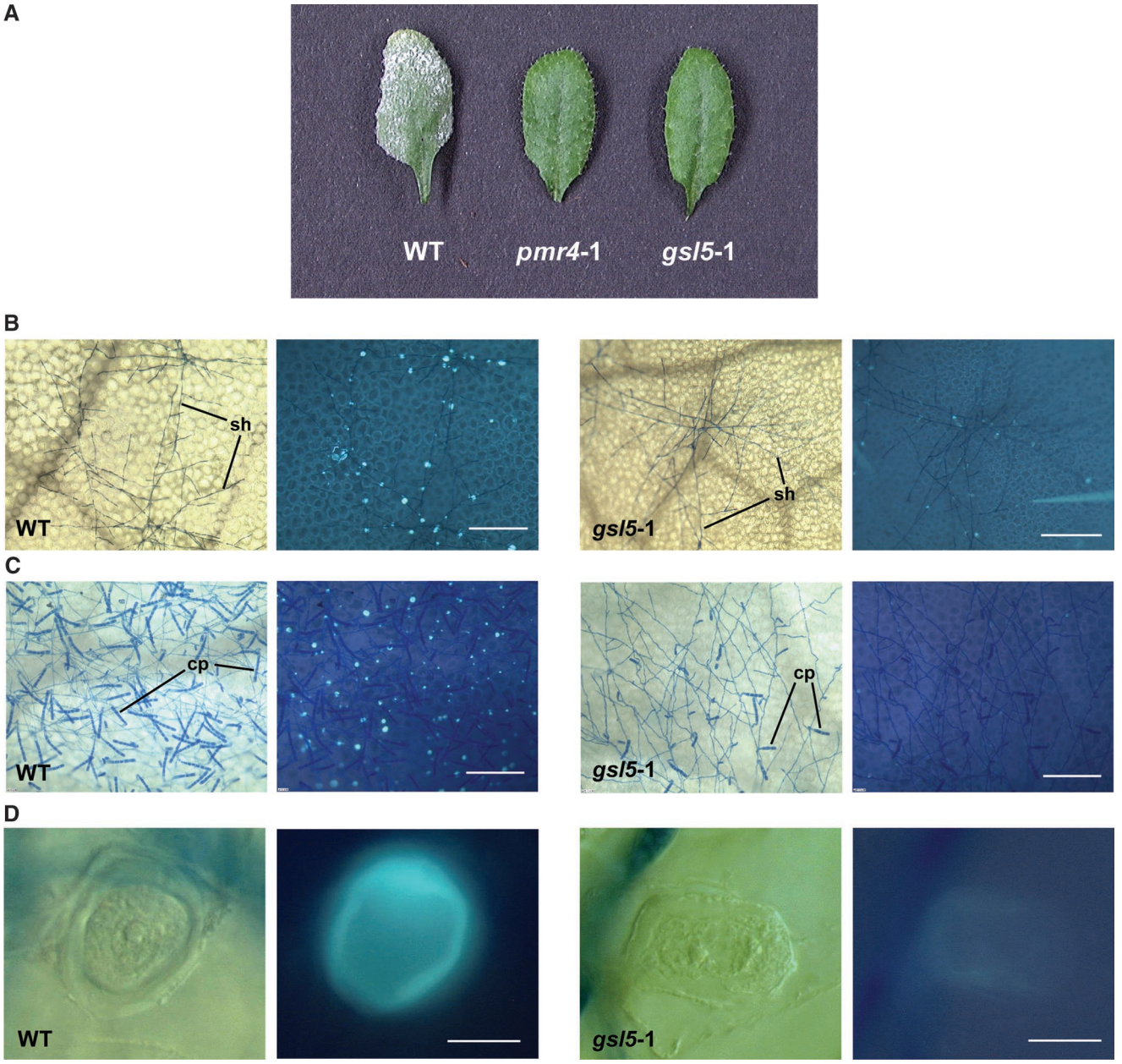

Figure 7. GSL5-Dependent Infection Phenotypes upon Challenge with the Powdery Mildew Fungus *G. orontii*.

Wild-type (WT) and T-DNA insertion (*gsl5-1*) plants were inoculated with *G. orontii* conidiospores.

(A) Single detached leaves from plants 10 days after inoculation. The surface of the leaf from the wild-type plant is covered by macroscopically visible hyphae, whereas mutants *pmr4-1* and *gsl5-1* develop no visible disease symptoms.

(B) Hyphal growth on the leaf surface at the commencement of callose encasement of haustorial complexes in wild-type and *gsl5-1* plants at 72 h after inoculation. A bright-field image is shown at left, and the corresponding fluorescence image after callose staining is shown at right. *gsl5-1* plants lack an intense aniline blue fluorochrome staining indicative of callose deposition at haustorial complexes. sh, secondary hyphae. Bars = 200 μm.

(C) A dense fungal mycelium and numerous conidiophores (cp) with long conidial chains as well as numerous local callosic deposits are visible on wild-type plants. A bright-field image is shown at left, and the corresponding fluorescence image after callose staining is shown at right. *gsl5-1* plants show significantly reduced conidiophore formation and shorter conidial chains. Bars = 200 μm.

(D) Higher magnification images of mature haustorial complexes encased by GSL5 callose from wild-type and *gsl5-1* plants. A bright-field image is shown at left, and the corresponding fluorescence microscopic image after callose staining is shown at right. Bars = 10 μm.

(Figure 7B, bright field). However, reduced hyphal growth and severely diminished conidiophore formation became detectable on *gsl5-1* leaves at 5 and 10 days after pathogen challenge (Figure 7C, bright field). This finding indicates that pathogen growth on the mutant plants is impaired significantly but is not inhibited completely. A striking encapsulation of haustorial complexes with callose was found in wild-type but not in *gsl5-1* leaves, suggesting that GSL5 participates in callose synthesis both in papillae and at haustoria before and after fungal entry into epidermal cells (Figure 7D). This encasement of haustorial complexes was recognizable as early as 72 h after spore inoculation (Figures 7B and 7C, epifluorescence). This finding corroborates our earlier observations of dynamic changes of GSL5 activity or location as the infection process progresses and might indicate a critical role for callose in the function of haustorial complexes.

DISCUSSION

To define potential roles of *GSL* genes in callose biosynthesis in plants, dsRNAi constructs that specifically target 3 of the 12 putative *GSL* genes in Arabidopsis—*GSL5*, *GSL6*, and *GSL11*—were used to generate stable transformants. Quantitative PCR showed that transcript levels of the three genes were reduced specifically in the dsRNAi transgenic lines. No evidence for compensatory upregulation of other *GSL* genes was detected. For example, in the *GSL5* lines, *GSL6* and *GSL11* mRNA remained at approximately the same levels as observed in the control and wild-type plants (data not shown). During the initial design of the dsRNAi constructs, regions in which sequences of >21 nucleotides were identical in any two different *AtGSL* genes were avoided (Hamilton and Baulcombe, 1999), but quantitative PCR showed some downregulation of *AtGSL* genes most closely related to the target genes (*AtGSL1*, *AtGSL3*, and *AtGSL7*, respectively; data not shown). Therefore, it was clear that the dsRNAi results would require independent confirmation through T-DNA insertion lines or other mutants in which a single gene had been disrupted. Although mRNA abundance for the specific *GSL* genes was lower in each of the corresponding dsRNAi transgenic lines, it was not abolished completely (Figure 1), presumably because dsRNAi silencing occurs post-transcriptionally (Fire et al., 1998) or because of potential cell type–specific differences in the activity of the 35S promoter, which drove the expression of the dsRNAi constructs (Sunilkumar et al., 2002).

In seeking a link between *GSL* expression and callose deposition, it was noticed initially that wound callose was reduced greatly, specifically in the *GSL5* dsRNAi plants (Figure 2). Wounding is an inherent consequence of fungal penetration of plant cells, so the effects of fungal challenge on the dsRNAi lines were examined. When the transgenic plants were challenged with several fungal species, the response of the dsRNAi *GSL5* lines differed markedly from that of the dsRNAi *GSL6*, dsRNAi *GSL11*, and control plants. In particular, papillary callose was absent in the dsRNAi *GSL5* line after inoculation of leaves with the fungal pathogens *S. fusca*, *G. orontii*, and *B. graminis*. Similar results were observed with the T-DNA insertion line GABI-KAT 089H05, in which the *GSL5* callose synthase gene is disrupted (Figure 6). As mentioned above, our focus was shifted from the dsRNAi lines to the homozygous GABI-KAT 089H05 T-DNA insertion line (*gsl5-1*). Although papillary callose was not detectable in *gsl5* plants, the typical round wall appositions that form beneath fungal appressoria, at least at the light microscopic level, were indistinguishable from those in wild-type plants except that they contained no callose (Figure 4C). Therefore, it seems unlikely that callose serves as an essential structural scaffold in papillae (cf. Smart et al., 1986; Bolwell, 1993). The formation of noncallosic papillae in *gsl5* plants indicates that the accumulation of papillary components other than callose continues.

The phenotypic characteristics of the *gsl5* lines were similar to those described for the powdery mildew–resistant *pmr4-1* mutant of Arabidopsis (Vogel and Somerville, 2000). We have shown here that the *pmr4-1* line has an internal stop codon in *GSL5* that is located in a similar position to the T-DNA insertion in the GABI-KAT 089H05 line in exon 2 of the gene (Figure 6). Based on a number of topology prediction programs, the lesions will disrupt the protein sequence close to the last transmembrane helix before the large, nonmembrane, and presumably cytoplasmic region of the protein that is widely assumed to contain the catalytic site (Figure 6) (Cui et al., 2001; Doblin et al., 2001; Hong et al., 2001a; Østergaard et al., 2002). It is highly unlikely that the truncated protein would have any callose synthase activity. Thus, our gene-silencing experiments and the mutant data clearly demonstrate a role for *AtGSL5* in the deposition of wound and papillary callose. More generally, the data provide strong genetic evidence that the products of *GSL* genes are essential for callose formation in higher plants.

It has long been believed that callosic papillae physically impede pathogen entry into plant cells, although this is not accepted universally (reviewed by Stone and Clarke, 1992). To test this hypothesis, we took advantage of a nonhost interaction phenotype between Arabidopsis and the grass powdery mildew fungus *B. graminis*, which is characterized by the failure of the pathogen to penetrate leaf epidermal cells on wild-type plants at most interaction sites (Figure 4A). Penetration incidence was only slightly higher in *gsl5* mutants, and infection did not occur. In other work, Arabidopsis mutants have been identified in which *B. graminis* penetration through the cell wall was increased dramatically, but none of these showed reduced callose formation at papillae (V. Lipka and P. Schulze-Lefert, unpublished data). Together, these observations indicate that resistance to wall penetration by the grass powdery mildew fungus is a plant-controlled process to which papillary callose does not contribute to any great extent. However, nonhost interactions with other fungal pathogens need to be tested on *gsl5* plants before we can generalize our observations with the *B. graminis* pathogen.

A striking finding in the present work was the different spatial and temporal accumulation patterns of GSL5 callose at different subcellular sites in single cells, namely at papillae and haustorial complexes, as well as along the entire cellular periphery after pathogen-provoked cell death (Figures 4 and 7). These changing patterns might reflect local stimulation of the activity of preexisting callose synthase enzyme or the specific targeting of newly synthesized enzyme to cellular "stress sites."

Each of the three pathogen-triggered GSL5 callose accumulation patterns is consistent with a plasma membrane location for the callose synthase, given that the extrahaustorial membrane is thought to be continuous with the plasma membrane (Giese et al., 1997; Mendgen and Hahn, 2002). At this stage, we favor the existence of a mechanism that mediates tight subcellular control of the activity of preexisting enzyme. The activity of plasma membrane–bound plant callose synthases often is dependent on Ca^{2+}, whereas in yeast, the Rho1 GTPase regulates the activity of the callose synthase homologs FKS1 and FKS2 by altering their phosphorylation status (Qadota et al., 1996; Calonge et al., 2003). A rapid increase in cytoplasmic free Ca^{2+} levels is a common response of plant cells to pathogen challenge (Blume et al., 2000; Grant et al., 2000) and wounding (Leon et al., 1998, 2001); therefore, it is conceivable that local increases in Ca^{2+} concentrations beneath fungal appressoria and at haustorial complexes contribute to local GSL5 stimulation. Subsequent increases in whole-cell cytoplasmic free Ca^{2+} levels after more widespread plasma membrane disintegration as the cell dies might contribute to GSL5 activation along the entire cell periphery.

Perhaps the most surprising observation with the *gsl5* lines is their enhanced resistance to attack by different biotrophic pathogens (Figure 7A). It was shown previously that the loss of *PMR4* function does not result in the constitutive expression of salicylic acid– or ethylene– and jasmonic acid–dependent defense pathways (Vogel and Somerville, 2000). Although Østergaard et al. (2002) showed salicylic acid–dependent *GSL5* gene expression, we have shown a link between GSL5 activity and wounding (Figure 2). Wounding of the cell wall is a feature of pathogenesis by biotrophic microorganisms that must enter plant cells for nutrient supply. Biotrophic pathogens such as *P. parasitica* and *E. cichoracearum* might have exploited components of the wound response for successful pathogenesis. It is conceivable that callose might be needed as a physical support for fungal development, either as a structural scaffold to accommodate haustorial complexes or to allow optimal nutrient uptake via this specialized feeding structure. Because cell wall penetration resistance was not altered substantially in the absence of callosic plugs and because haustorium differentiation was not impaired in any detectable manner upon challenge with the tested virulent pathogens in *gsl5* leaves (Figure 7D), a structural role of GSL5 callose for "intracellular" accommodation of fungal infection structures seems unlikely.

However, GSL5 callose might either facilitate nutrient uptake by haustoria or serve as a pathogen-induced protection barrier that prevents the recognition of pathogen-derived molecules by the host. For example, lack of callose might unmask fungal wall polysaccharides and/or secreted proteins. Certain branched (1→3,1→6)-β-D-oligoglucosides and chitin/chitosan oligosaccharides released from these fungal wall polysaccharides (Bartnicki-Garcia, 1968) by partial endohydrolysis are highly active elicitors of plant defense responses, even at concentrations as low as 10 nM (Côté and Hahn, 1994). By contrast, linear (1→3)-β-D-oligoglucosides of the type that would be released from callose itself by the (1→3)-β-D-glucanases are not active in eliciting plant defense (Côté and Hahn, 1994). The evolution of (1→3)-β-D-glucanase inhibitors by pathogenic fungi implies that inhibiting the release of (1→3,1→6)-β-D-oligoglucosides could be important for the establishment of fungal infection (Rose et al., 2002).

METHODS

Plant Lines and Growth Conditions

The *Arabidopsis thaliana GSL5* T-DNA insertion line GABI-KAT 089H05 was provided by Bernd Weisshaar (Max-Planck-Institute for Plant Breeding Research) and had been generated in the GABI-Kat program (http://www.mpiz-koeln.mpg.de/GABI-Kat/GABI-Kat_homepage.html). Oligonucleotide sequences used for T-DNA insertion detection were 5′-CGCAGATGCTGCATATAA-3′ and 5′-CAGTATAGTTAGTTAGAAATAATCC-3′ (GSL5 specific and T-DNA left border specific, respectively).

The powdery mildew–resistant line *pmr4-1* was obtained from John Vogel and Shauna Somerville (Carnegie Institution of Washington, Stanford, CA). Plants were transformed by the floral-dip method (Clough and Bent, 1998) using *Agrobacterium tumefaciens* strain GV3101::pMP90(RK) with the binary vectors pAJ5, pAJ6, and pAJ7. T3 plants used in infection experiments were grown in a glasshouse at 22°C. Seedlings (10 days old) transformed with double-stranded RNA interference (dsRNAi) constructs were selected by spraying every second day for 1 week with 100 mg/L Basta (AgrEvo, Düsseldorf, Germany).

dsRNAi Constructs

Gene-specific inverted repeats separated by an intron were inserted into plasmid pJawohl3 (AF404854) to create pAJ5 (*GSL6*; At1g05570), pAJ6 (*GSL11*; At3g59100), and pAJ7 (*GSL5*; At4g03550) dsRNAi constructs. Primer combinations used to produce the gene-specific sense and antisense *GSL* dsRNAi fragments were as follows: for *AtGSL5*, 5′-CATCGATGGGATCCGTACTGTCT-3′/5′-GGAAGGGACGGAAGCTTGAATTC-3′ and 5′-GGAAGGCCCGGGATGTTGGATTG-3′/5′-CGGCGTTGGTGTCCGTACTAGT-3′ (230-bp product); for *AtGSL6*, 5′-CATCGATAAAGGATCCCATACACCGTAA-3′/5′-CATCCATGGGATTAAGCTTCCCGGGCCA-3′ and 5′-CATCCATGGGATTAAGCTTCCCGGGCCA-3′/5′-CCGTCCATAAAGGATCCCATACACTAGT-3′ (640-bp product); and for *AtGSL11*, 5′-TGGGAAGCTTGGTGGAACGTAGA-3′/5′-TGACTGACAAGGATCCGAGGAAGAG-3′ and 5′-TGGGATCCGTGGTGGAATTCAGA-3′/5′-TGACTAGTAAAAACTCGAGGAAGAGA-3′ (280-bp product).

DNA and RNA Extractions

Genomic DNA was extracted from young leaves of Arabidopsis using the hot cetyl-trimethyl-ammonium bromide method (Lassner et al., 1989). Total RNA was extracted from young leaves and inflorescences of dsRNAi lines using the Trizol reagent (Invitrogen, Carlsbad, CA) according to the manufacturer's instructions.

Quantitative PCR Analysis of *GSL* mRNA

Total RNA (5 μg) was used in cDNA reactions using the Superscript II cDNA synthesis kit (Invitrogen). The cDNA was diluted 2.5-fold, and 1 μL was taken for quantitative real-time PCR in 20-μL reaction volumes using 10 μL of 2× Quanti-Tect PCR master mix (Qiagen, Valencia, CA), 0.3 μM gene-specific primers, and 0.6 μL of a 100-fold dilution of SYBR Green I dye (Applied Biosystems, Foster City, CA). PCR cycling and fluorescence measurements were performed with a Rotorgene 2000 Real-Time Cycler RG2072 (Corbett, Sydney, Australia), and data were normalized against glyceraldehyde phosphate dehydrogenase (*GAPDH*), actin (*Actin1*), and cyclophilin (*Cyclo*) mRNA levels (Vandesompele et al.,

2002). Primers used in the quantitative PCR were as follows: for AtGAPDH (At3g26650), 5′-TGGTTGATCTCGTTGTGCAGGTCTC-3′/5′-GTCAGCCAAGTCAACAACTCTCTG-3′; for AtActin1 (At2g37620), 5′-TGCGACAATGGAACTGGAATG-3′/5′-GGATAGCATGTGGAAGTGCATAC-3′; for AtCyclo (At2g36130), 5′-TGGCGAACGCTGGTCCTAATACA-3′/5′-CAAAAACTCCTCTGCCCCAATCAA-3′; for AtGSL5 (At4g03550), 5′-CTGGAATGCTGTTGTCTCTGTTG-3′/5′-TCGCCTTTTGATTTCTTCCCAGT-3′; for AtGSL6 (At1g05570), 5′-GAAGGGTTTGGGCGTTGGAAG-3′/5′-CAATGAGAAGCATTCCCCATCCAGTT-3′; and for AtGSL11 (At3g59100), 5′-TTTAGGGGTTTGGGACTCGGTGAAA-3′/5′-TGTCTTTCCGACCAGCGAGAATCA-3′.

Sequence Analysis of *PMR4-1*

The three exons of *GSL5* (1870, 2022, and 1448 bp, respectively) were amplified by PCR using flanking oligonucleotide primers. Purified PCR products (NucleoSpin extraction kit; Macherey-Nagel, Düren, Germany) were subjected to direct DNA sequencing. DNA sequences were determined by the MPIZ DNA core facility on Applied Biosystems (Weiterstadt, Germany) ABI Prism 377 and 3700 sequencers using BigDye-terminator chemistry. Forward/reverse primers used for *GSL5* exon amplification and sequencing from *pmr4-1* and *gsl5-1* plants were as follows: Exon1, 5′-ATTGTTTCTTCAGTGAAGCT-3′/5′-TCAAGTCAAGCGTTGTAC-3′; Exon2, 5′-CGCAGATGCTGCATATAA-3′/5′-CAGTATAGTTAGTTAGAAATAATCC-3′; and Exon3, 5′-GGATTATTTCTAACTAACTATACTG-3′/5′-GAACAAGGAGCTTTACCGT-3′. Additional sequencing primers were as follows: Exon1b-F, 5′-GTAAGTGGAGGAACTACGA-3′; Exon1b-R, 5′-AGCCAGGATTTCGGGCACC-3′; and Exon2b-F, 5′-GATTCTCACCTCTAGGGAC-3′.

Wounding

Four- to 6-week-old plants were wounded by cutting leaves with a razor. After 24 h, the leaves were detached, cleared, and stained for callose accumulation.

Pathogenicity Assays

The formation of callosic plugs was examined in 4- to 6-week-old plants 48 h after inoculating leaves with spores from the powdery mildew fungus *Sphaerotheca fusca*. Four- to 6-week-old Arabidopsis plants were inoculated with spores of *Golovinomyces orontii* and *Blumeria graminis* as described previously (Peterhänsel et al., 1997; Vogel and Somerville, 2000).

Microscopic Analyses

Tissue fixation and staining of fungal structures and callose were performed as described previously (Peterhänsel et al., 1997; Vogel and Somerville, 2000). Tissues were examined with a Zeiss Axioplan 20 fluorescence microscope (Carl Zeiss, Oberkochen, Germany). Epi-illumination was used at an excitation cutoff limit of 365 nm with barrier filter KP620.

Upon request, materials integral to the findings presented in this publication will be made available in a timely manner to all investigators on similar terms for noncommercial research purposes. To obtain materials, please contact Paul Schulze-Lefert, schlef@mpiz-koeln.mpg.de.

ACKNOWLEDGMENTS

We thank John Vogel and Shauna Somerville for providing the *pmr4-1* line, Neil Shirley for assistance with the quantitative PCR experiments, and Bruce Stone for helpful suggestions. This work was supported by grants from the Grains Research and Development Corporation and the Australian Research Council (to G.B.F.) and from the Max Planck Society (to P.S.-L.).

Received August 6, 2003; accepted September 12, 2003.

REFERENCES

Bartnicki-Garcia, S. (1968). Cell wall chemistry, morphogenesis, and taxonomy of fungi. Annu. Rev. Microbiol. **22,** 87–108.

Bestwick, C.S., Brown, I.R., Bennett, M.H.R., and Mansfield, J.W. (1997). Localization of hydrogen peroxide accumulation during the hypersensitive reaction of lettuce cells to *Pseudomonas syringae* pv *phaseolicola*. Plant Cell **9,** 209–221.

Blume, B., Nuernberger, T., Nass, N., and Scheel, D. (2000). Receptor-mediated increase in cytoplasmic free calcium required for activation of pathogen defense in parsley. Plant Cell **12,** 1425–1440.

Bolwell, G.P. (1993). Dynamic aspects of the plant extracellular matrix. Int. Rev. Cytol. **146,** 261–323.

Braun, U., Cook, R.T.A., Inman, A.J., and Shin, H.D. (2002). The taxonomy of the powdery mildew fungi. In The Powdery Mildews, R. Bélanger, A.J. Dik, and W.R. Bushnell, eds (St. Paul, MN: American Phytopathological Society Press), pp. 13–54.

Brown, I., Trethowan, J., Kerry, M., Mansfield, J., and Bolwell, G.P. (1998). Localization of components of the oxidative cross-linking of glycoproteins and of callose synthesis in papillae formed during the interaction between non-pathogenic strains of *Xanthomonas campestris* and French bean mesophyll cells. Plant J. **15,** 333–343.

Cabib, E., Roh, D.-H., Schmidt, M., Crotti, L.B., and Varma, A. (2001). The yeast cell wall and septum as paradigms of cell growth and morphogenesis. J. Biol. Chem. **276,** 19679–19682.

Calonge, T.M., Arellano, M., Coll, P.M., and Perez, P. (2003). Rga5p is a specific Rho1p GTPase-activating protein that regulates cell integrity in *Schizosaccharomyces pombe*. Mol. Microbiol. **47,** 507–518.

Clough, S.J., and Bent, A.F. (1998). Floral dip: A simplified method for *Agrobacterium*-mediated transformation of *Arabidopsis thaliana*. Plant J. **16,** 735–743.

Côté, F., and Hahn, M.G. (1994). Oligosaccharins: Structures and signal transduction. Plant Mol. Biol. **26,** 1379–1411.

Cui, X.J., Shin, H.S., Song, C., Laosinchai, W., Amano, Y., and Brown, R.M. (2001). A putative plant homolog of the yeast β-1,3-glucan synthase subunit FKS1 from cotton (*Gossypium hirsutum* L.) fibers. Planta **213,** 223–230.

Dijkgraaf, G.J., Abe, M., Ohya, Y., and Bussey, H. (2002). Mutations in Fks1p affect the cell wall content of β-1,3- and β-1,6-glucan in *Saccharomyces cerevisiae*. Yeast **19,** 671–690.

Doblin, M.S., De Melis, L., Newbigin, E., Bacic, A., and Read, S.M. (2001). Pollen tubes of *Nicotiana alata* express two genes from different β-glucan synthase families. Plant Physiol. **125,** 2040–2052.

Donofrio, N.M., and Delaney, T.P. (2001). Abnormal callose response phenotype and hypersusceptibility to *Peronospora parasitica* in defense-compromised Arabidopsis nim1-1 and salicylate hydroxylase-expressing plants. Mol. Plant-Microbe Interact. **14,** 439–450.

Douglas, C.M., et al. (1994). The *Saccharomyces cerevisiae Fks1* (*Etg1*) gene encodes an integral membrane protein which is a subunit of (1→3)-β-D-glucan synthase. Proc. Natl. Acad. Sci. USA **91,** 12907–12911.

Fire, A., Xu, S., Montgomery, M.K., Kostas, S.A., Driver, S.E., and Mello, C.C. (1998). Potent and specific genetic interference by double-stranded RNA in *Caenorhabditis elegans*. Nature **391,** 806–811.

Giese, H., Hippe-Sanwald, S., Somerville, S., and Weller, J. (1997). Plant relationships. In The Mycota V, Part B, G. Carroll and P. Tudzynski, eds (Heidelberg, Germany: Springer), pp. 55–78.

Grant, M.R., Brown, I., Adams, S., Knight, M., Ainslie, A., and Mansfield, J.W. (2000). The *RPM1* plant disease resistance gene facilitates a rapid and sustained increase in cytosolic calcium that is necessary for the oxidative burst and hypersensitive cell death. Plant J. **23,** 441–450.

Hamilton, A.J., and Baulcombe, D.C. (1999). A species of small antisense RNA in posttranscriptional gene silencing in plants. Science **286,** 950–952.

Heath, M.C. (1998). Involvement of reactive oxygen species in the response of resistant (hypersensitive) or susceptible cowpeas to the cowpea rust fungus. New Phytol. **138,** 251–263.

Heath, M.C. (2002). Cellular interactions between biotrophic fungal pathogens and host or nonhost plants. Can. J. Plant Pathol. **24,** 259–264.

Hong, Z.L., Delauney, A.J., and Verma, D.P.S. (2001a). A cell plate–specific callose synthase and its interaction with phragmoplastin. Plant Cell **13,** 755–768.

Hong, Z.L., Zhang, Z.M., Olson, J.M., and Verma, D.P.S. (2001b). A novel UDP-glucose transferase is part of the callose synthase complex and interacts with phragmoplastin at the forming cell plate. Plant Cell **13,** 769–779.

Itaya, A., Woo, Y.M., Masuta, C., Bao, Y., Nelson, R.S., and Ding, B. (1998). Developmental regulation of intercellular protein trafficking through plasmodesmata in tobacco leaf epidermis. Plant Physiol. **118,** 373–385.

Kobayashi, Y., Kobayashi, I., Funaki, Y., Fujimoto, S., Takemoto, T., and Kunoh, H. (1997). Dynamic reorganization of microfilaments and microtubules is necessary for the expression of non-host resistance in barley coleoptile cells. Plant J. **11,** 525–537.

Lassner, M.W., Palys, J.M., and Yoder, J.I. (1989). Genetic transactivation of dissociation elements in transgenic tomato plants. Mol. Gen. Genet. **218,** 25–32.

Leon, J., Rojo, E., and Sanchez, S.J.J. (2001). Wound signalling in plants. J. Exp. Bot. **52,** 1–9.

Leon, J., Rojo, E., Titarenko, E., and Sanchez, S.J.J. (1998). Jasmonic acid-dependent and -independent wound signal transduction pathways are differentially regulated by Ca^{2+}/calmodulin in *Arabidopsis thaliana*. Mol. Gen. Genet. **258,** 412–419.

Mendgen, K., and Hahn, M. (2002). Plant infection and the establishment of fungal biotrophy. Trends Plant Sci. **7,** 352–356.

Northcote, D.H., Davey, R., and Lay, J. (1989). Use of antisera to localize callose, xylan and arabinogalactan in the cell-plate, primary and secondary walls of plant cells. Planta **178,** 353–366.

Østergaard, L., Petersen, M., Mattsson, O., and Mundy, J. (2002). An Arabidopsis callose synthase. Plant Mol. Biol. **49,** 559–566.

Peterhänsel, C., Freialdenhoven, A., Kurth, J., Kolsch, R., and Schulze-Lefert, P. (1997). Interaction analyses of genes required for resistance responses to powdery mildew in barley reveal distinct pathways leading to leaf cell death. Plant Cell **9,** 1397–1409.

Qadota, H., Python, C.P., Inoue, S.B., Arisawa, M., Anraku, Y., Zheng, Y., Watanabe, T., Levin, D.E., and Ohya, Y. (1996). Identification of yeast Rho1p GTPase as a regulatory subunit of (1→3)-β-D-glucan synthase. Science **272,** 279–281.

Richmond, T.A., and Somerville, C.R. (2000). The cellulose synthase superfamily. Plant Physiol. **124,** 495–498.

Rose, J.K.C., Ham, K.S., Darvill, A.G., and Albersheim, P. (2002). Molecular cloning and characterization of glucanase inhibitor proteins: Coevolution of a counterdefense mechanism by plant pathogens. Plant Cell **14,** 1329–1345.

Ryals, J.A., Neuenschwander, U.H., Willits, M.G., Molina, A., Steiner, H.Y., and Hunt, M.D. (1996). Systemic acquired resistance. Plant Cell **8,** 1809–1819.

Smart, M.G., Aist, J.R., and Israel, H.W. (1986). Structure and function of wall appositions. 1. General histochemistry of papillae in barley (*Hordeum vulgare*) coleoptiles attacked by *Erysiphe graminis* f. sp. *hordei*. Can. J. Bot. **64,** 793–801.

Stone, B.A., and Clarke, A.E. (1992). Chemistry and Biology of (1→3)-β-D-Glucans. (Victoria, Australia: La Trobe University Press).

Stone, B.A., Evans, N.A., Bonig, I., and Clarke, A.E. (1985). The application of Sirofluor, a chemically defined fluorochrome from aniline blue for the histochemical detection of callose. Protoplasma **122,** 191–195.

Sunilkumar, G., Mohr, L., Lopata, F.E., Emani, C., and Rathore, K.S. (2002). Developmental and tissue-specific expression of CaMV 35S promoter in cotton as revealed by GFP. Plant Mol. Biol. **50,** 463–474.

Thordal-Christensen, H., Zhang, Z., Wei, Y., and Collinge, D.B. (1997). Subcellular localization of H_2O_2 in plants: H_2O_2 accumulation in papillae and hypersensitive response during the barley-powdery mildew interaction. Plant J. **11,** 1187–1194.

Vandesompele, J., De Preter, K., Pattyn, F., Poppe, B., Van Roy, N., De Paepe, A., and Speleman, F. (2002). Accurate normalisation of real-time quantitative RT-PCR data by geometric averaging of multiple internal control genes. Genome Biol. **3,** 1–12.

Verma, D.P.S., and Hong, Z.L. (2001). Plant callose synthase complexes. Plant Mol. Biol. **47,** 693–701.

Vogel, J., and Somerville, S. (2000). Isolation and characterization of powdery mildew-resistant Arabidopsis mutants. Proc. Natl. Acad. Sci. USA **97,** 1897–1902.

NOTE ADDED IN PROOF

During the processing of this manuscript, Nishimura et al. (**Nishimura, M.T., Stein, M., Hou, B.H., Vogel, J.P., Edwards, H., and Somerville, S.C.** [2003]. Loss of a callose synthase results in salicylic acid-dependent disease resistance. Science **301,** 969–972) published work on Arabidopsis *pmr4* mutants. They showed that PMR4 encodes GSL5 callose synthase and demonstrated that resistance to powdery mildew infection is mediated through the salicylic acid pathway.